Cone-beam Reconstruction using Limited EPID Projections for Seeds Localization

Jina Chang*, Won-Kyun Jung*, Sung-Ho Park†, Kwang-Ho Cheong‡, Tae-Suk Suh*

*Department of Biomedical Engineering, The Catholic University of Korea, †Department of Radiation Oncology, Asan Medical Center, University of Ulsan, ‡Department of Radiation Oncology, Halym University Sacred Heart Hospital, Seoul, Korea

In this study, we describe the preliminary application for the delineation of a metal object using cone-beam reconstruction (CBR) based on limited electronic portal imaging device (EPID) projections. A typical Feldkamp, Davis and Kress (FDK) reconstruction algorithm accompanying the edge preserving smoothing filter was used as only a few projections are acquired for reconstruction. In a correlation study of the projection numbers, we found that the size of the seeds and their location depicted by these CBR images were almost identical. Limited views were used for CBR, and our method is inexpensive and competitive for use in clinical applications.

Key Words: Cone-beam reconstruction, Limited EPID projections, Seeds localization

INTRODUCTION

Recently, on-board cone-beam CT has been widely used for image-guided radiation therapy applications.[1-3] However, the scatter radiation can degrade the quality of a kilovoltage cone-beam computed tomography (KV CBCT) image due to the use of a larger flat-panel detector. Especially with the use of KV CBCT for metal object visualization, the effect of streak metal artifacts can be magnified in CBCT images. There are many metal artifact reduction techniques for KVCT images using segmentation,[4,5] filtering,[6] and sinogram subtraction.[7] However, the use of these techniques can be troublesome, because these works were case-by-case solutions for most clinical applications. A megavoltage cone-beam CT (MV CBCT) image may be a simple solution for reducing the severe image artifacts in the region of high atomic number seeds. Descovich *et al.*[8] reported a localization method using MVCT scans, and these images were used to complement KVCT images where metal artifacts exist. However, the use of two complete imaging sets is not practical and the use of two complete imaging sets could increase the patient dose.

In this approach, using cone-beam reconstruction (CBR) based on limited electronic portal imaging device (EPID) projections, we could delineate a metal object for better localization.

MATERIALS AND METHODS

1. Experimental setup

The KV cone-beam CT and EPID projection data was acquired with a Trilogy linear accelerator (Varian Medical Systems, Palo Alto, CA USA) that was integrated in the on-board imager (OBI). Instrumentation consisted of a kV-source and flat-panel combination mounted on the drum of a medical accelerator. The CBCT data was acquired in full-fan mode using the OBI system. The EPID based MV CBR experiments were performed with a 6 MV beam and a-Si flat-panel detector. The beam delivery was one monitor unit (MU) per image, with a 6-degree interval of gantry location.

As the linear accelerator (linac) system included the KV CBCT imaging system and linac treatment beam at a 90-degree gap, theoretically, the two image sets have a same

This research sponsored by the Nuclear R&D Program of the Ministry of Science and Technology (M20706000007-07M0600-00710) and Seoul Research and Business Development Program (10550).
Submitted April 17, 2008, Accepted September 5, 2008
Corresponding Author: Tae-Suk Suh, Department of Biomedical Engineering, The Catholic University of Korea, 505, Banpo-dong, Seocho-gu, Seoul 137-701, Korea.
Tel: 02)590-2420, Fax: 02)532-1779
E-mail: suhsanta@catholic.ac.kr

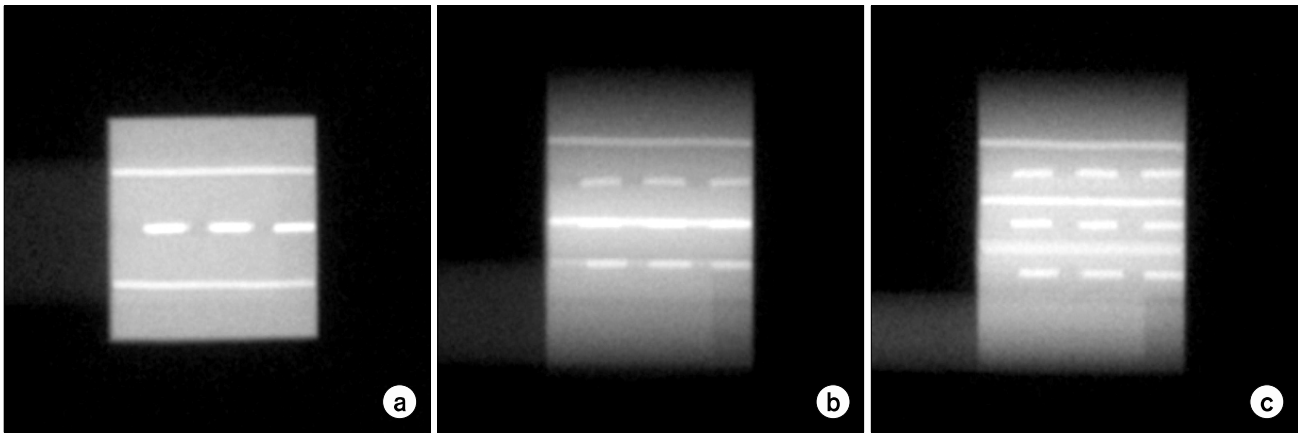

Fig. 1. EPID projection views from the test phantom at (a) 0°, (b) 45°, and (c) 60°.

isocenter coordinates.

The test phantom was used for evaluating our algorithm. Fig. 1 shows the EPID projection images at 0°, 45°, 60° from the test phantom. The size of the phantom was 50×50×50 mm, and the diameter of the brass metal wire was 2 mm; the lengths were 10 mm and 50 mm.

2. CBR from a limited EPID view

A typical Feldkamp, Davis and Kress (FDK) reconstruction algorithm[9] accompanying the edge preserving smoothing filter was used. First, a bilateral filter[10] was applied to the EPID projection images to reduce noise while maintaining the seeds edge details as only a few projections are acquired for reconstruction. Then, the CBR algorithm was applied.

1) The bilateral filtering: The filter was applied by replacing the current value of a focal pixel with the bilaterally weighted sum of pixels. The bilateral filter can be expressed as

$$h(x,y) = k^{-1}(x,y) \int_{-\infty}^{\infty}\int_{-\infty}^{\infty} f(x+i, y+j)c(i+j)s(x,y,i,j)didj \quad (1)$$

where,

$$c(i+j) = e^{-\frac{(i^2+j^2)}{2\sigma_d^2}} \quad (2)$$

$$s(x,y,i,j) = e^{-(\frac{(I(x+i,j+j)-I(x,y))^2}{2\sigma_r^2}} \quad (3)$$

$$k(x,y) = \int_{-\infty}^{\infty}\int_{-\infty}^{\infty} c(i+j)s(x,y,i,j)didj \quad (4)$$

The output intensity of a focal pixel $h(x,y)$ is the sum of the Gaussian function $c(i+j)$ and the similarity function $s(x,y,i,j)$ when the input intensity of the neighborhood pixel $f(x+i, y+j)$ is applied. $k^{-1}(x,y)$ is a normalization factor, and σ_d, σ_r determine the amount of Gaussian filtering and combination of pixel values.

2) FDK algorithm: The FDK algorithm is based on filtering and back projection of the single planes and the result is obtained by summing up the contributions of all tilted fan beams. The FDK algorithm is expressed as follows:

$$f(x,y,z) = \int_0^{2\pi} \frac{1}{U^2} Q_\beta(a(x,y,\beta), b(x,y,z,\beta),\beta)d\beta \quad (5)$$

where,

$$s = xcos\beta + ysin\beta,\ t = -xcos\beta + ysin\beta \quad (6)$$

$$U = \frac{D-s}{D} \quad (7)$$

$$a(x,y,\beta) = \frac{tD}{D-s} \quad (8)$$

$$b(x,y,z,\beta) = \frac{zD}{D-s} \quad (9)$$

The reconstructed voxels $f(x,y,z)$ is the sum over all projection angles β of the filtered projection $Q_\beta(a,b,\beta)$ multiplied by a weighted projection $\frac{1}{U^2}$ for the flat detector. D is the distance between the source and the origin.

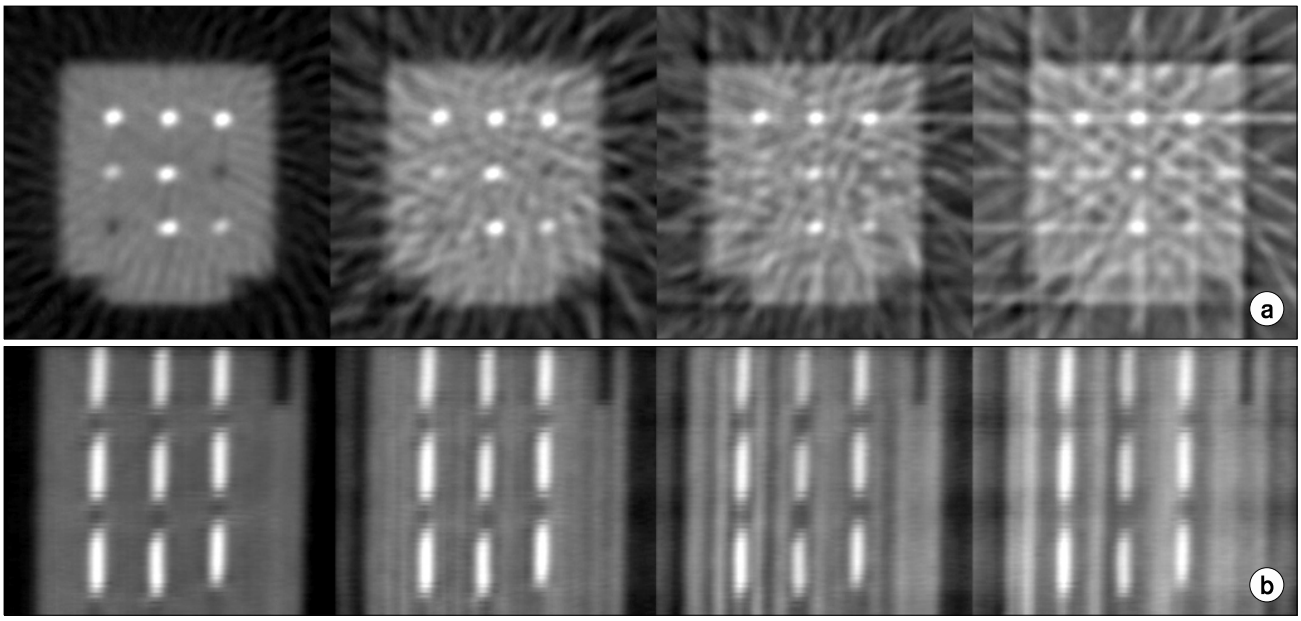

Fig. 2. CBR images using limited projections (a) 60, 30, 20 and 12 projections in axial views (b) 60, 30, 20 and 12 projections in coronal views.

3. Evaluation

To quantify seed evaluation according to the number of projections, we compared the FWHM (full width at half maximum) of the metal wires. After format conversion to downscale the image data, the horizontal and vertical line profiles were generated at the maximum signal intensity in each coronal view. These values were then normalized to the metal seed intensity of the CBR image from 120 EPID projections. In addition to the FWHM, the seeds profiles were measured to evaluate a consistency of the seeds reconstruction image.

RESULTS

Fig. 2 shows the images that were reconstructed using limited 60, 30, 20, and 12 EPID projections in an axial and coronal view. Although image quality was poor in soft-tissue regions, the metal wires were clearly demonstrated as a strong signal intensity spot. Tables 1 and 2 list the FWHM values of the vertical and horizontal lines in the coronal view. The FWHM of middle seed from the 20 projections in the Table 2 shows lower value compare to the other seeds. The one pixel difference made a large FWHM difference, because the FWHM calculated in the small seed length of 2 mm (6 pixels). However, in a correlation study of projection numbers, we found that the size of the seeds and their location depicted by these CBR images were almost identical. A distinct density difference between seeds and surrounding materials was a

Table 1. The FWHM values of vertical lines in the coronal view (normalized to a CBR image from 120 projections).

FWHM	Number of projections			
	60	30	20	12
Upper seed	1.12	1.12	1.12	1.48
Middle seed	1.00	1.00	1.00	1.32
Lower seed	1.00	1.07	1.07	1.32

Table 2. The FWHM values of horizontal lines in the coronal view (normalized to a CBR image from 120 projections).

FWHM	Number of projections			
	60	30	20	12
Left seed	1.13	1.13	1.13	1.50
Middle seed	1.00	1.17	0.67	1.00
Right seed	1.00	1.14	1.14	1.71

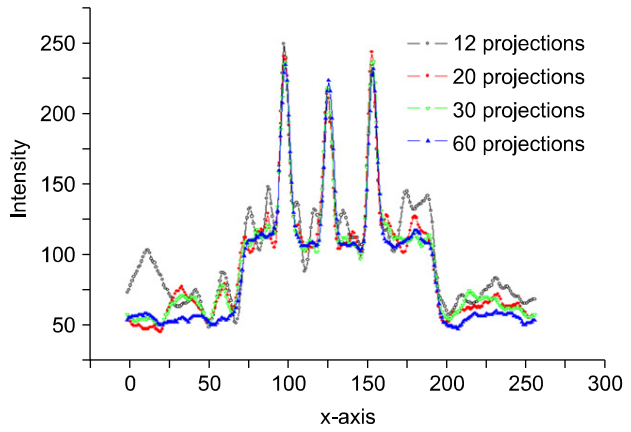

Fig. 3. Seeds profiles of the horizontal line in the coronal view.

main cause of these results. If the surrounding material has a high density composition such as bone, the result may different. Fig. 3 shows the seeds profiles of the horizontal lines in the coronal view. As can be seen, the pixel intensity tends to have higher fluctuations as the number of projections were decreased.

DISCUSSION

The amount of scattered radiation in CBCT causes a degradation of the image quality and magnification of the metal artifact. With this approach, the EPID views of the treatment beam were used for complementation of the delineation of metal objects. Highly sensitive and automated on-board EPID now utilizes MV CBCT imaging. The MV CBCT system employs the MV source of the linac and the EPID for imaging. A strong point for use of this system is a simple hardware requirement and geometric coincidence with the treatment beam.[11] Moreover, due to the development of the Si detector, the EPID was used for absolute[12] and relative dosimetry.[13,14] The MV CBCT was also used for dose calculations after calibration of uniformity-corrected MV CBCT15. However, MV CBCT imaging included a high imaging dose (typically 1～5 cGy) and the low visibility of large low-contrast objects.

In the KV CBCT environment, we additionally used EPID projections for the demonstration of metallic objects. Limited views were used for CBR and our method is inexpensive and is competitive for use in clinical applications.

CONCLUSION

We have demonstrated the use of EPID views in conjunction with a CBR algorithm. In this study, a typical FDK algorithm was used for CBR. Preliminary results with a phantom have demonstrated effectiveness of the procedure to demonstrate metallic objects. However, when the cone angle becomes larger, the FDK algorithm degrades the image quality. Thus, further improvements still can be made with an application of various CBR algorithm for better seeds localization.

REFERENCES

1. **Jaffray D, Siewerdsen J, Wong J, Martinez A**: Flat-panel cone-beam computed tomography for image-guided radiation therapy. Int J Radiat Oncol Biol Phys 53:1337-1349 (2002)
2. **Hawkins M, Brock K, Eccles C, Moseley D, Jaffray D, Dawson L**: Assessment of residual error in liver position using kV cone-beam computed tomography for liver cancer high-precision radiation therapy. Int J Radiat Oncol Biol Phys 66:610-619 (2006)
3. **Thilmann C**: Correction of patient positioning errors based on in-line cone beam CTs: clinical implementation and first experiences. Radiat Oncol 1:16 (2006)
4. **Yu H, Zeng K, Bharkhada DK, et al**: A segmentation-based method for metal artifact reduction. Acad Radiol 14:495-504 (2007)
5. **Zhang Y, Zhang L, Zhu XR, Lee AK, Chambers M, Dong L**: Reducing metal artifacts in cone-beam CT images by preprocessing projection data. Int J Radiat Oncol Biol Phys 67: 924-932 (2007)
6. **Bal M, Spies L**: Metal artifact reduction in CT using tissue-class modeling and adaptive prefiltering. Med Phy 33: 2852-2859 (2006)
7. **Takahashi Y, Mori S, Kozuka T, et al**: Preliminary study of correction of original metal artifacts due to I-125 seeds in postimplant dosimetry for prostate permanent implant brachytherapy. Radiation Medicine 24:133-138 (2006)
8. **Descovich M, Morin O, Aubry J, et al**: Megavoltage cone-beam CT to complement CT-based treatment planning for HDR brachytherapy. Brachytherapy 5:85-86 (2006)
9. **Feldkamp LA, Davis LC, Kress JW**: Practical cone-beam algorithm. J Opt Soc Am A 1:612-619 (1984)
10. **Tomasi C, Manduchi R**: Bilateral filtering for gray and color images. Proceedings of the 1998 IEEE International Conference on Computer Vision 839-846 (1998)
11. **Pouliot J, Bani-Hashemi A, Chen J, et al**: Low-dose megavoltage cone-beam CT for radiation therapy. Int J Radiat Oncol Biol Phys 61:552-560 (2005)

12. **Pasma KL, Heijmen BJM, Kroonwijk M, Visser AG**: Portal dose image (PDI) prediction for dosimetric treatment verification in radiotherapy. I. An algorithm for open beams. Med Phys 25:830-840 (1998)
13. **El-Mohri Y, Antonuk LE, Yorkston J, et al**: Relative dosimetry using active matrix flat-panel imager (AMFPI) technology. Med Phys 26:1530-1541 (1999)
14. **Chang J, Mageras GS, Chui CS, Ling CC, Lutz W**: Relative profile and dose verification of intensity modulated radiation therapy. Int J Radiat Oncol Biol Phys 47:231-240 (2000)
15. **Morin O, Chen J, Aubin M, et al**: Dose calculation using megavoltage cone-beam CT. Int J Radiat Oncol Biol Phys 67:1201-1210 (2007)

Seed의 위치 확인을 위한 제한된 EPID 영상을 이용한 콘빔 재구성

*가톨릭대학교 의과대학 의공학교실, †서울아산병원 방사선종양학과, ‡한림대학교성심병원 방사선종양학과

장지나*・정원균*・박성호†・정광호‡・서태석*

본 연구에서는 금속 물체의 묘사를 위한 예비 연구로서 제한된 EPID 영상을 이용한 콘빔 재구성을 수행하였다. 콘빔 재구성에 제한된 영상이 이용되었기 때문에 일반적인 FDK 재구성 알고리즘에 에지 보존 평활화(edge preserving smoothing) 필터가 사용되었다. 사용된 영상의 수와의 상관관계를 비교해 보았을 때 금속 seed의 크기와 위치에 대한 결과는 거의 동일하다고 판명되었다. 콘빔 CT 재구성을 위하여 제한된 영상을 사용하였기 때문에 우리의 방법은 임상 적용에 있어 경제적이고, 효과적인 방법이 될 수 있을 것으로 사료된다.

중심단어: 콘빔 재구성, 제한된 EPID 영상, Seed 위치 검증